

An experimental study on prevention of saline wedge intrusion by an air curtain in rivers

Etude expérimentale de la prévention de l'intrusion d'un coin salé en rivière par un rideau d'air

MASANORI NAKAI and MASAMITSU ARITA, *Department of Civil and Environmental Engineering, Tokyo Denki University, Hatoyama-machi, Hiki-gun, Saitama, Japan*

ABSTRACT

Prevention of saline wedge intrusion by an air curtain in rivers was experimentally studied from a physical viewpoint. The behavior of steady saline wedges around an air curtain was classified into the three types and their appearance conditions were clearly expressed by the two parameters A/B and A/R : A , B , and R represent the buoyancy due to an air curtain, the intrusion force of a saline wedge, and the inertial force of a fresh water flow (a river flow), respectively. In addition, the effectiveness of this method was evaluated using the newly introduced parameter α defined by $(A/B)/(A/R)$.

RÉSUMÉ

La prévention d'une intrusion saline en rivière, par un rideau d'air, a été étudiée expérimentalement d'un point de vue physique. Le comportement des coins salés permanents autour d'un rideau d'air a été classé en trois types et les conditions de leur apparition ont été clairement exprimées à l'aide des deux paramètres A/B et A/R : A , B , et R représentant respectivement, la force d'Archimède due à un rideau d'air, la force intrusive du coin salé, et la force d'inertie de l'écoulement d'eau douce (une rivière). De plus, l'efficacité de cette méthode a été évaluée à l'aide du paramètre α nouvellement introduit, défini par $(A/B)/(A/R)$.

Key Words: Saline wedge, Air curtain, Flow mechanism, Flow type classification

1. Introduction

Saline wedge intrusion into rivers damages agriculture in their neighboring regions through water intake troubles. The most suitable means to solve or reduce this problem has been considered to shorten intrusion length of saline wedges, and a lot of studies on this respect have been carried out. Of various methods to prevent saline wedge intrusion, a method in which a mound or a weir is built on a channel bottom is thought to have both drastic effectiveness and a serious defect: the latter is that the flood run-off capability of a river channel will greatly decrease. A method through the use of an air curtain has a possibility to be an alternative one. It would be superior to the former method in rivers with narrow width, because construction and maintenance of an air curtain maker are relatively easy, and the flood run-off capability does not decrease. In addition, this method has another advantage: oxygen in river water will increase by dissolving of air bubbles. Abraham and Burgh(1964) initially used an air curtain to prevent the progress of a density current induced by a lock exchange flow. Sasaki and Asaeda(1993) also performed a similar experiment to examine the flow mechanism around an air curtain. Asaeda et al.(1997) carried out numerical and experimental studies for the same flow. They reported that the numerical model qualitatively reproduced the flow field and also presented the flow type classification based on their experimental results. However, the results were quantitatively inadequate. The three studies have some weaknesses in application to natural rivers, because there are the essential differences in the flow mechanisms between density current intrusion induced by a lock exchange flow

and saline wedge intrusion. On the other hand, Komatsu et al.(1996) conducted a field investigation on the effects of an air curtain in the River Sendai in Japan. In spite of the above studies, the effectiveness of the air curtain method has not been sufficiently clarified associated with the flow mechanism.

In this study, we experimentally treated the behavior of steady saline wedges in the presence of an air curtain and attempted to make clear the flow mechanism around an air curtain. In addition, we discussed the hydraulic conditions in which an air curtain works most effectively. 'Air curtain', in this study, expresses a line (two-dimensional) upward air bubble flow which is perpendicular to the streamwise direction of a river or a channel.

2. Experimental apparatus and procedure

A two-dimensional straight channel which is 1200 (cm) in length, 5 (cm) in width, and 20 (cm) in height was used in this experiment (see Fig. 1(a)). A fresh water flow ran from the upstream side to the downstream side in the channel, and its depth was controlled by the overflow equipped in the downstream tank. Saline wedge intrusion was reproduced in the channel by release of salt water from the outlet placed at the downstream edge (the junction between the channel and the downstream tank) to the upstream side, and its discharge (per unit width) q_s was set to larger values than the values which correspond to the natural river condition^{*}). A circular cylinder was used as a model of an air curtain maker and was laid on the channel bottom, being perpendicular to the streamwise direction of the channel, at the point 1.6 (m) upstream from the downstream edge. The model is 0.8 (cm) in diameter

Revision received November 3, 2000. Open for discussion till October 31, 2002.

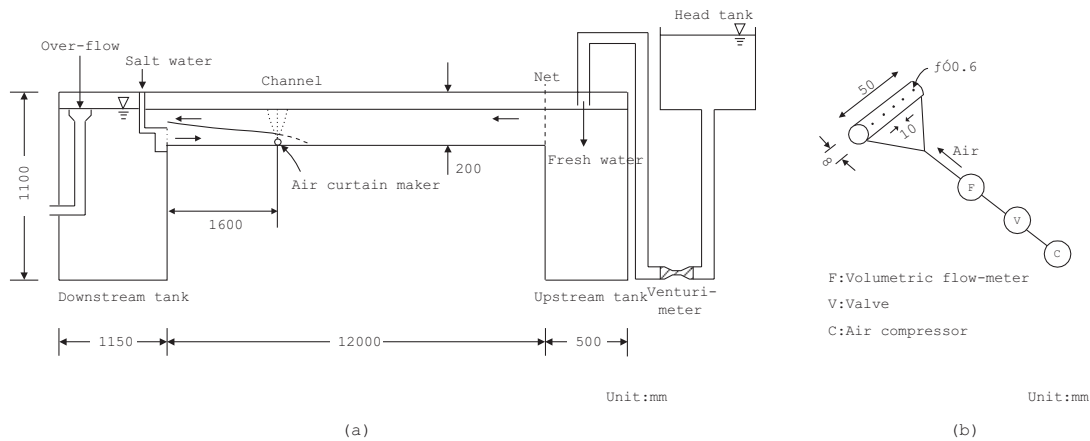


Fig. 1 Experimental apparatus used. (a) Channel (side view). (b) Model of the air curtain maker

and 5.0 (cm) in length with small holes (diameter $d = 0.6(\text{mm})$) in every 1.0 (cm) in its axial direction. Air was transported to the model using an air compressor through a small tube via a flow-meter (see Fig. 1(b)). The air bubble size (diameter) d_a was fixed to about 3.0-5.0(mm)**), and the coalescence and split of air bubbles were not observed.

Table 1 shows the experimental conditions. The discharge per unit width of a fresh water flow q_f and the density of salt water ρ_s were changed in every case, on the other hand, the total water depth H and the density of fresh water ρ_f were fixed as almost same in all cases. The discharge per unit width of air bubbles at the standard atmospheric pressure q_a was variously changed in each case. Re_o and F_o are the channel Reynolds number and channel densimetric Froude number respectively and are defined as,

$$Re_o = \frac{q_f}{\nu} \quad (1)$$

$$F_o = \frac{q_f}{(g'H^3)^{\frac{1}{2}}} \quad (2)$$

Where, g' and ν denote the buoyancy acceleration and the kinematic viscosity respectively. In addition, g' is equal to $\Delta\rho g/\rho_f$, $\Delta\rho(=\rho_s - \rho_f)$ is the difference in density between salt water and fresh water, and g is the gravitational acceleration.

In the experiment, first, a steady saline wedge was produced in the absence of an air curtain in the channel. Second, an air curtain was formed by release of air bubbles from the model. Then, the flow behavior around the air curtain was observed and photographed, and the longitudinal thickness profile of the saline wedge all over the channel was measured, in a steady state.

Fig. 2 depicts the schematic diagram of the definitions of the symbols used in this study. In this figure, h_1 , h_2 , L , and x represent the thicknesses of a fresh water flow and a saline wedge, the saline wedge length, and the distance from the downstream edge, respectively. The definitions of other symbols in this figure were previously mentioned.

Case	q_f (cm^2/s)	ρ_f (g/cm^3)	ρ_s (g/cm^3)	H (cm)	q_a (cm^2/s)	Re_o	F_o
Case-1	40.6	0.9994	1.0032	15.9	0~2.05	4100	0.33
Case-2	50.6	0.9994	1.0073	16.0	0~3.33	5100	0.28
Case-3	60.2	0.9996	1.0102	16.1	0~4.15	6000	0.29
Case-4	80.0	0.9998	1.0103	16.2	0~2.49	8000	0.38
Case-5	20.2	0.9998	1.0034	15.7	0~3.32	2000	0.17
Case-6	20.5	1.0000	1.0070	15.8	1.25~4.17	2000	0.12
Case-7	19.8	0.9999	1.0106	15.8	2.09~3.35	2000	0.10
Case-8	20.0	0.9990	1.0044	15.7	0.82~4.10	2000	0.14
Case-9	30.6	0.9986	1.0036	15.8	1.22~2.86	3100	0.22
Case-10	30.9	0.9984	1.0019	15.8	0.81~4.06	3100	0.27
Case-11	11.6	0.9986	1.0037	15.6	1.23~2.05	1200	0.08

*1) q_f and q_a express discharges per unit width.

*2) q_f was measured using a Venturi-meter.

*3) ρ_s was measured using an electric density-meter.

*4) q_a was measured using a volumetric flow-meter.

*) In reproduction of saline wedge intrusion in the channel, the salt water discharge q_s should be equalized to the discharge q_{se} which satisfies the boundary condition at a river mouth: $F_1^2 + F_2^2 = I$ (F_1 and F_2 are the densimetric Froude numbers in the upper and lower layers respectively). In the experiment, however, we set q_s to larger values than q_{se} to avoid the lack of salt water supply, and the surplus salt water directly return to the downstream tank without intrusion.

***) In the additional experiment, the effects of the air bubble size d_a on the phenomenon were investigated in the ranges of $0.2(\text{mm}) \leq d_a \leq 2.0(\text{mm})$, $0.5(\text{mm}) \leq d_a \leq 2.4(\text{mm})$, $0.6(\text{mm}) \leq d_a \leq 2.9(\text{mm})$, and $3.0(\text{mm}) \leq d_a \leq 5.0(\text{mm})$. The significant change of the phenomenon by a variation in d_a was not observed in these ranges. In the case of micro-bubbles, however, the phenomenon will significantly change.

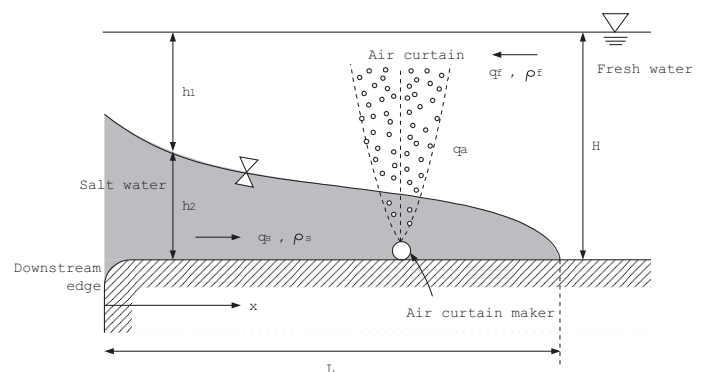


Fig. 2 Definition sketch

3. Results and discussion

3.1 Shape and length of saline wedges

We introduce some examples of the experimental results to show the effects of an air curtain for prevention of saline wedge intrusion. Fig. 3 shows the variation of a shape of a saline wedge with the change of the air bubble discharge q_a for Case 2. In this figure, Type I and Type II express the flow types defined in the following section (see the figure's caption). This figure represents that saline wedge intrusion is somewhat suppressed for $q_a=0.83(\text{cm}^2/\text{s})$, and that the saline wedge is completely arrested at the air curtain's location for $q_a \geq 2.29(\text{cm}^2/\text{s})$.

Fig. 4 depicts the relationship between the air bubble discharge q_a and the saline wedge length L in Case 1, 2, 5, and 6. This figure gives us the minimum values of q_a in which the saline wedges can be completely arrested at the air curtain's location for Case 1, 2, and 5. In Case 6, in contrast, although the air curtain can greatly reduce the saline wedge length, it cannot completely prevent saline wedge intrusion. In addition, this case exhibits an interesting phenomenon: the saline wedge length L becomes larger with an increase in q_a in the range of $q_a \geq 2.5(\text{cm}^2/\text{s})$. The reason for this phenomenon will be discussed later.

3.2 Flow mechanism and flow type classification

Saline wedges in a channel variously behave by the influence of an air curtain as shown in Figs. 3 and 4, and their behavior can be classified into the three types: Type I, II, and III, as illustrated in Fig. 5. Photo. 1(a), (b), and (c) show the visualized side views of the flow patterns (Type I, II, and III) around the air curtain. In these photographs, salt water masses are seen black-colored by dye, and the left-hand and right-hand sides correspond to the downstream and upstream sides of the channel respectively.

Type I expresses a type in which salt water masses intrude into the upstream side over an air curtain along a channel bottom. This type appears, when the kinetic energy converted from the buoy-

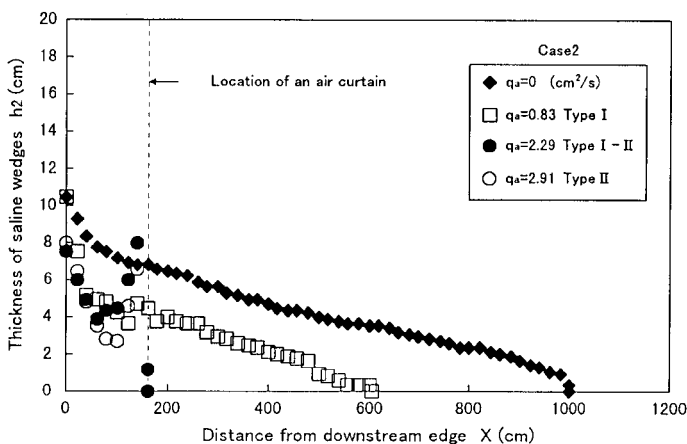


Fig. 3 Variation of a shape of a saline wedge with the air bubble discharge q_a : Type I and Type II in the legend represent the flow types defined as Fig.5 in the section 3-2. Type I-II expresses the transient behavior between Type I and Type II.

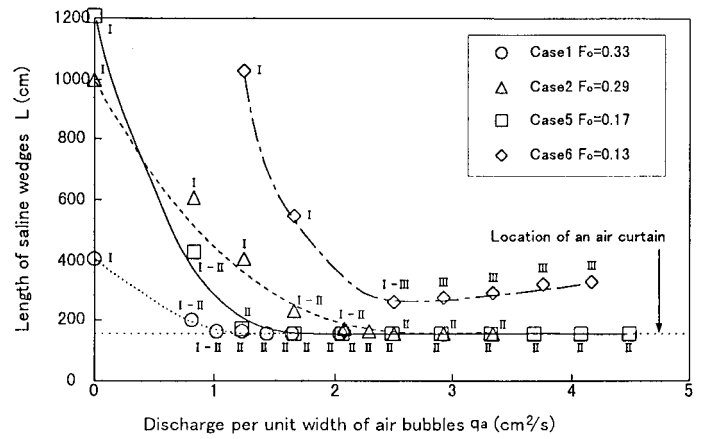


Fig. 4 Relationship between the air bubble discharge q_a and the saline wedge length L : The symbols I, II, and III indicate Type I, Type II, and Type III, respectively (see Fig.5). The symbols I-II and I-III express the transient behavior between Type I and Type II and that between Type I and Type III, respectively.

ancy due to an air curtain in the upward flow is small. Therefore, only a small amount of salt water masses can be lifted up. In Type II, all salt water masses rise up to the water surface by the strong upward flow triggered by the buoyancy due to an air curtain and return to the downstream side being influenced by the fresh water flow. In this type, saline wedge intrusion can be completely prevented by an air curtain. In Type III, also, all salt water masses rise up to the water surface, however, their certain portions enter the upstream side of an air curtain forming convection and then run to the upstream side along a channel bottom again.

Herein, we discuss the flow mechanism of the three flow types. The external forces dominating the phenomenon are thought to be the following three: the buoyancy due to an air curtain A , the intrusion force of a saline wedge B , and the inertial force of a fresh water flow (a river flow) R . All the three parameters can be written in a dimension of velocity as follows,

$$A = (q_a g)^{\frac{1}{3}} \quad (3)$$

$$B = (g' h_a)^{\frac{1}{2}} \quad (4)$$

$$R = \frac{q_f}{H} \quad (5)$$

Where, h_a represents the saline wedge thickness at the position of the air curtain maker, however, it is a value in the absence of an air curtain.

First, let us consider the flow driven by an air curtain in the absence of salt water intrusion. An air curtain makes an upward jet which impinges on the water surface. After the impingement, the jet spreads near the water surface being influenced by the fresh water flow, and its characteristic depends on the relative relation between A and R . With large A/R , the jet spreads to the both sides of the air curtain near the water surface. In addition, weak convection (a weak circulating flow) is produced, in the upstream

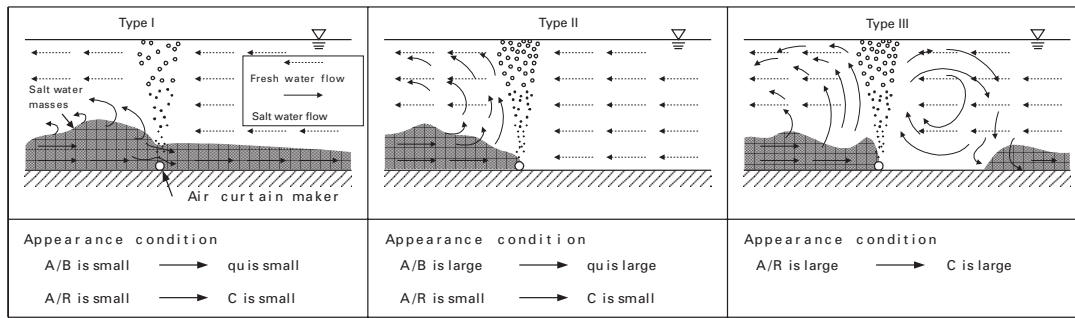


Fig. 5 Flow type classification

side of the air curtain, by the interaction between the bubble-driven upward jet and the fresh water flow (see the left figure in Fig. 6(a)). On the other hand, with small A/R , it spreads only to the downstream side because of the strong fresh water flow (see the left figure in Fig. 6(b)).

Second, we discuss the behavior of salt water masses running from the downstream side around an air curtain. When A/B is large, all the salt water masses can be lifted up to the water surface, being mixed with the bubble-driven upward jet, by the strong buoyancy due to an air curtain; the rising discharge of salt water q_u will be large. After that, their behavior depends on A/R . If A/R is small, all of them returns to the downstream side being influenced by the downstream flow turning from the upward jet and the fresh water flow (see the right figure in Fig. 6(b)). Accordingly, the flow behavior will be Type II. On the other hand, if A/R is large, certain portions of the salt water masses lifted up enter the upstream side of an air curtain with the upstream flow turning from the upward jet and run over the weak circulating flow. The circulating flow is intensified by the salt water flow surrounding it, and then, a distinct convection cell is produced in the upstream side (see the right figure in Fig. 6(a)). Consequently, the circulation of the convection cell C becomes a certain large

value, and the flow behavior will be Type III.

When A/B is small, some of salt water masses intrude into the upstream side of an air curtain along a channel bottom because of the weak buoyancy due to an air curtain. In this case, the rising discharge of salt water q_u yields small, and the flow behavior will be Type I in cases in which A/R is small. While, Type III appears in cases in which A/R is large, because a distinct convection cell is formed in the upstream side of an air curtain by the salt water flow surrounding the weak circulating flow (in this study, Type III includes cases in which salt water masses enter the upstream side of an air curtain forming a convection cell simultaneously with running over an air curtain along a channel bottom).

Fig. 7 shows the schematic diagram concerning the above discussion. It can be summarized that the behavior of a saline wedge around an air curtain depends both on A/B and A/R . A/B governs the rising discharge of salt water by an air curtain q_u ; q_u increases with an increase in A/B , while, A/R dominates the formation of the convection cell in the upstream side of an air curtain; its circulation C increases with an increase in A/R . In another way, the behavior of a saline wedge around an air curtain is determined both by q_u and C .

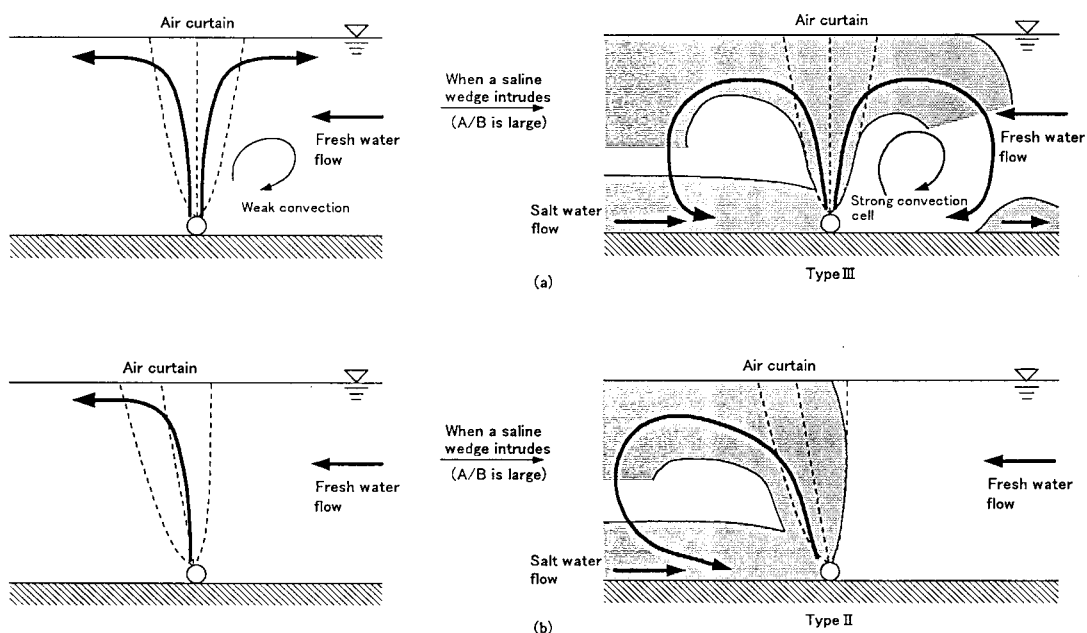


Fig. 6 Flow driven by an air curtain and the behavior of salt water masses around an air curtain. (a) In cases of large A/R . (b) In cases of small A/R

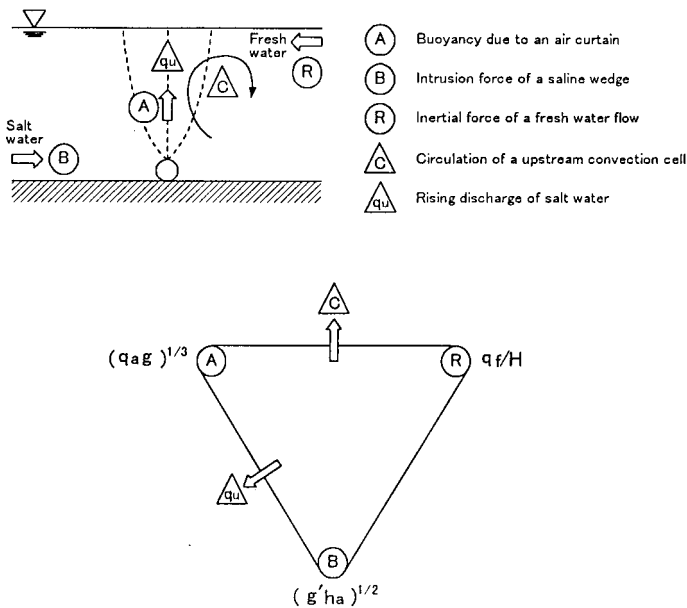


Fig. 7 Factors governing the phenomenon and their relationship

3.3 Appearance conditions of Type I, II, and III and effectiveness of an air curtain

Fig. 8 shows the appearance conditions of Type I, II, and III by A/R and A/B . Herein, the slopes of the solid lines (a , b) and the dot-dash line are represented by α defined by the following equation.

$$\alpha = \frac{A/B}{A/R} = \frac{R}{B} = F_o \left(\frac{h_a}{H} \right)^{-1/2} \quad (6)$$

The domains of Type I, II, and III are clearly divided in this figure. This means that A/R and A/B are the suitable parameters for the discussion of the appearance conditions of the flow types. From this figure, we can also understand that Type I appears in the region where both A/R and A/B are small, and that the domains of Type II and Type III are separated by the dot-dash line with the slope $\alpha = 0.21$. The solid line (a) expresses that the flow type varies from Type I to Type II with increasing q_a in the range of $\alpha > 0.21$. On the other hand, the solid line (b) shows that the

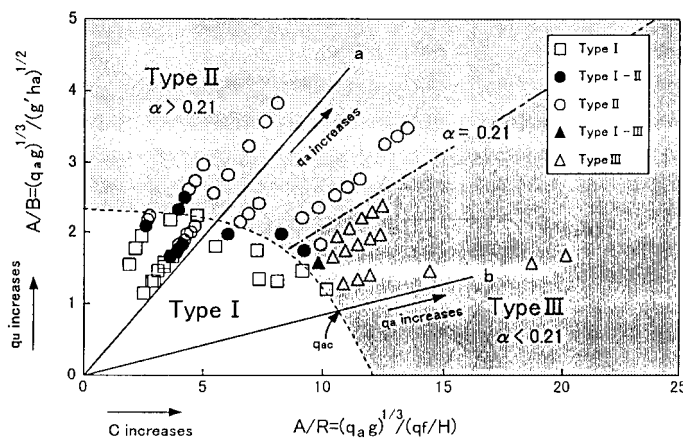


Fig. 8 Appearance conditions of Type I, II, and III expressed by A/R and A/B

flow type changes from Type I to Type III with increasing q_a in the range of $\alpha < 0.21$. In Fig. 4, Case 1, 2, and 5, and Case 6 correspond to the former and latter cases respectively.

Let us consider the effectiveness of an air curtain for prevention of saline wedge intrusion from Fig. 8. Type II appears with an increase in q_a under the condition of $\alpha > 0.21$, and then, an air curtain can completely arrest saline wedges and will work most effectively. While, Type I or III appears under the condition of $\alpha < 0.21$, and then, an air curtain cannot completely prevent saline wedge intrusion. However, an air curtain makes it possible to shorten saline wedge length largely, thus, it can contribute to reduction of saline wedge intrusion and seems to be effective in an engineering aspect.

In the use of an air curtain under the condition of $\alpha < 0.21$, we have to pay attention to the following. The saline wedge length tends to be shorter with an increase in q_a for Type I, however, this tendency will reverse for Type III (Case 6 in Fig. 4 corresponds to this case). This is because, in Type III, an increase in C (the circulation of the upstream convection cell) according to an increase in q_a accelerates the salt water re-intrusion along a channel bottom in the upstream side of the convection cell. Accordingly, under the condition of $\alpha < 0.21$, the suitable air bubble discharge q_{ac} which minimizes the saline wedge length exists and coincides with q_a at the boundary between Type I and Type III.

From the above discussion, it was made clear that the effectiveness of an air curtain for prevention of saline wedge intrusion in various cases could be judged by the value of α . In application of Fig. 8 to natural rivers, F_o and H are commonly provided from fields, and h_a which is often difficult to be obtained from fields can be determined using one of some established mathematical models on saline wedge intrusion (for instance, Arita and Jirka (1987)). Consequently, the value of α will be calculated from eq. (6) for natural rivers, from this respect, it can be said that this study has certain practicability.

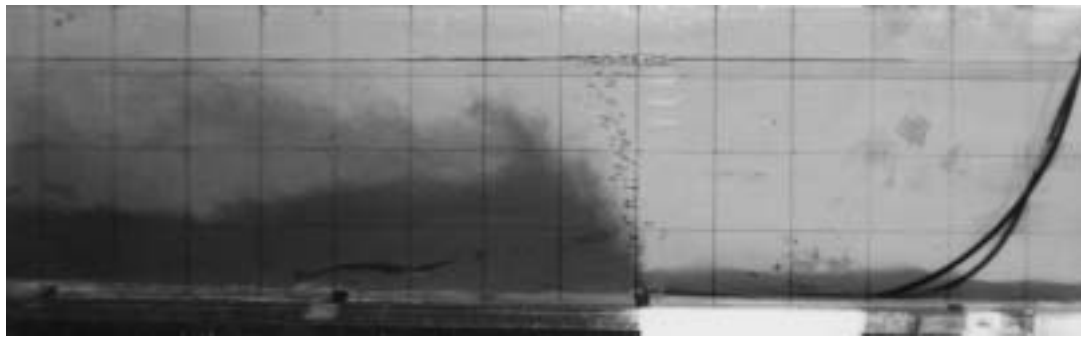
In natural rivers, R_{eo} also plays an important role in saline wedge intrusion. In Fig. 8, although the effects of R_{eo} are partially included through h_a/H (h_a/H changes with a variation in R_{eo} ; see Arita and Jirka(1987) which presents the great effects of R_{eo} on the behavior of saline wedges), it seems to be insufficient, because R_{eo} in this experiment is restricted in the narrow range: $1.2 \times 10^3 \leq R_{eo} \leq 8.0 \times 10^3$ (see Table 1). Additional investigations for various R_{eo} should be carried out by large scale experiments or field works.

In addition, as previously mentioned, we fixed the air bubble size d_a to about 3.0-5.0(mm) in this experiment. The effects of d_a on the phenomenon should be examined over the wide range of d_a , including the case of micro-bubbles, in future studies.

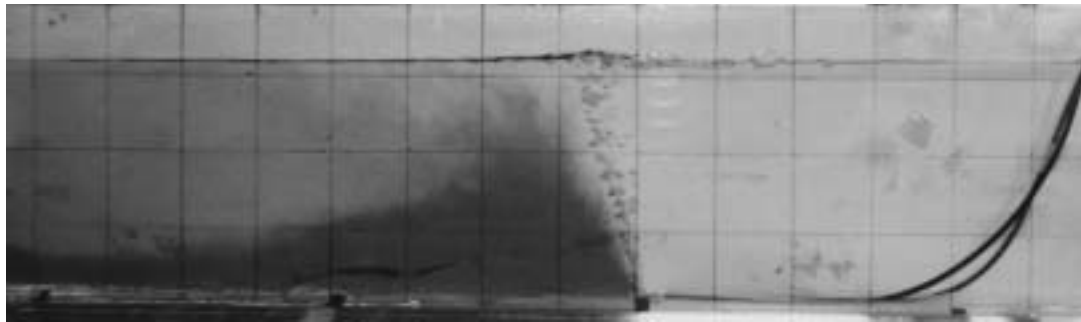
4. Concluding remarks.

In this study, the behavior of steady saline wedges in the presence of an air curtain was experimentally investigated introducing a new physical concept. The concluding remarks obtained are as follows.

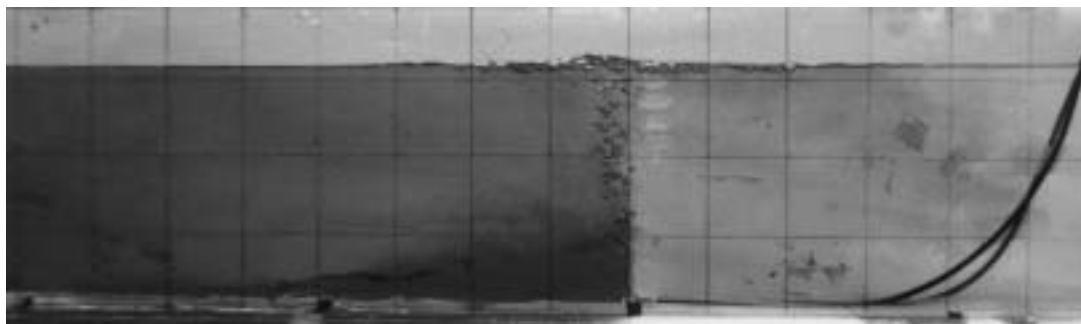
- (1) Saline wedges variously behave around an air curtain being governed by the three external forces: the buoyancy due to



(a)



(b)



(c)

Photo 1. Examples of Type I, II, and III (side views). (a) Type I (Case 2: $q_a = 1.25 \text{ (cm}^2/\text{s)}$). (b) Type II (Case 2: $q_a = 2.91 \text{ (cm}^2/\text{s)}$). (c) Type III (Case 6: $q_a = 3.33 \text{ (cm}^2/\text{s)}$).

an air curtain A , the intrusion force of a saline wedge B , and the inertial force of a fresh water flow (a river flow) R . Their behavior can be classified into the three types: Type I, II, and III, and their appearance conditions are clearly expressed by A/R and A/B .

- (2) In Type II, an air curtain completely prevents saline wedge intrusion and works most effectively. This type appears in cases in which the newly introduced parameter α is greater than 0.21 and the air bubble discharge q_a is greater than the certain value. Both in Type I and Type III, in contrast, an air curtain cannot completely arrest saline wedges at its position. However, the intrusion length of saline wedges largely decreases, thus, the air curtain method has certain effectiveness even in these types.

Acknowledgement

We would like to express our special thanks to one of the reviewers for his valuable comments. One of his comments is that an air curtain may be more effective at large scales being based on the non-linear relation between the buoyancy due to an air curtain and the converted kinetic energy in the upward flow. Another is the suggestion of the use of a water curtain in place of an air curtain. Both the comments are very valuable and will be our future problems.

References

- ABRAHAM, G. and BURGH, P.V.D. (1964), Pneumatic reduction of salt intrusion through locks., Jour. Hydr. Div., ASCE, Vol.90, No.HY1, pp.83-119.

- ARITA, M. and JIRKA, G.H. (1987), Two-layer model of saline wedge, I and II., Jour. Hydr. Engrg., ASCE, Vol.113, No.10, pp.1229-1263.
- ASAEDA, T., ARITA, M. and PHAM, H.D. (1997), Prevention of saline wedge intrusion by an air curtain in an estuary., Jour. Hydr., Coastal and Environ. Engrg., JSCE, No.572/ II-40, pp.23-31 (in Japanese).
- KOMATSU, T., UESUGI, T., ADACHI, T., MATSUOKA, H., SAKAMOTO, K., YAMATO, N. and ASADA, M. (1996), Artificial control of salt water intrusion in the River Sendai., Proc. Coastal Engrg., JSCE, Vol.43, pp.341-345 (in Japanese).
- SASAKI, T. and ASAEDA, T. (1993), Mechanism of prevention of salt water intrusion by an air curtain in a river., Proc. Environ. Systems, JSCE, Vol.21, pp.335-339 (in Japanese).

Notations

The following symbols are used in this paper.

- A buoyancy due to an air curtain
- B intrusion force of a saline wedge
- C circulation of the upstream convection cell
- d diameter of the holes for air bubble release in the air curtain maker
- d_a diameter of air bubbles

- F_o channel densimetric Froude number
- g gravitational acceleration
- g' buoyancy acceleration(= $\Delta\rho g/\rho_f$)
- H total water depth
- h_a thickness of a saline wedge at the position of the air curtain maker (a value in the absence of an air curtain)
- h_1 thickness of a fresh water flow
- h_2 thickness of a saline wedge
- L length of a saline wedge
- q_a discharge per unit width of air bubbles
- q_{ac} discharge per unit width of air bubbles at the boundary between Type I and Type III (see Fig. 8)
- q_f discharge per unit width of a fresh water flow
- q_s discharge per unit width of a salt water flow
- q_u rising discharge of salt water by an air curtain
- R inertial force of a fresh water flow (a river flow)
- R_{eo} channel Reynolds number
- x distance from the downstream edge of the channel
- α newly introduced parameter (= $(A/B)/(A/R)$)
- $\Delta\rho$ difference in density between salt water and fresh water (= $\rho_s - \rho_f$)
- ν kinematic viscosity
- ρ_f density of fresh water
- ρ_s density of salt water